

Cell-Specific Retrograde Signals Mediate Antiparallel Effects of Angiotensin II on Osmoreceptor Afferents to Vasopressin and Oxytocin Neurons

Tevye J. Stachniak,^{1,2} Eric Trudel,¹ and Charles W. Bourque^{1,*}

¹Centre for Research in Neuroscience, Research Institute of the McGill University Health Centre, Montreal, QC H3G1A4, Canada

²Discovery Neuroscience, F. Hoffman-La Roche AG, Basel 4051, Switzerland

*Correspondence: charles.bourque@mcgill.ca

<http://dx.doi.org/10.1016/j.celrep.2014.06.029>

This is an open access article under the CC BY-NC-ND license (<http://creativecommons.org/licenses/by-nc-nd/3.0/>).

SUMMARY

Homeostatic control of extracellular fluid osmolality in rats requires a parallel excitation of vasopressin (VP) and oxytocin (OT) neurosecretory neurons by osmoreceptor afferents to regulate the amount of water and sodium in the urine under normal conditions. However, during decreased blood volume (hypovolemia), natriuresis is suppressed, whereas osmotically driven antidiuresis is enhanced to promote retention of isotonic fluid. Because Angiotensin II (Ang II) is released centrally to indicate hypovolemia, we hypothesized that Ang II can evoke a state-dependent switch in circuit function. Here, we show that Ang II, a neuropeptide released centrally during hypovolemia, suppresses osmoreceptor-mediated synaptic excitation of OT neurons while potentiating excitation of VP neurons. Ang II does this by inducing cell-autonomous release of nitric oxide by VP neurons and endocannabinoids by OT neurons to respectively enhance and reduce glutamate release by osmoreceptor afferents. These findings indicate that peptide modulators such as Ang II can regulate synaptic communication to achieve a state-dependent and target-specific modulation of circuit activity.

INTRODUCTION

Mammals strive to maintain a constant extracellular fluid (ECF) osmolality to avoid the traumatic consequences of brain swelling or shrinking caused by acute osmotic stress. Central homeostatic networks regulate salt and water balance through the principle of negative feedback, whereby small osmotic perturbations detected by osmosensory neurons, such as those in the OVLT (*organum vasculosum laminae terminalis*), drive proportional homeostatic responses through the activation of downstream effector neurons (Bourque, 2008). Specifically, increases in ECF osmolality proportionally enhance the spontaneous action potential firing rate of OVLT neurons (Ciura and Bourque, 2006), which causes a corresponding increase in glutamatergic

synaptic excitation of magnocellular neurosecretory neurons (MNCs) in the supraoptic nucleus (SON), whereas GABAergic transmission is unchanged (Richard and Bourque, 1995). The resulting increase in vasopressin (VP) and oxytocin (OT) secretion into the bloodstream mediates a robust osmoregulatory response because VP (antidiuretic hormone) produces urinary water retention (Robertson et al., 1976) and OT causes sodium excretion (natriuresis) (Verbalis et al., 1991). Therefore, a proportional and parallel modulation of the osmosensory OVLT to VP neuron pathway (OVLT → SON_{VP}) and OVLT to OT neuron pathway (OVLT → SON_{OT}) is required for the maintenance of ECF osmolality.

In contrast, ECF volume regulation commonly requires an opposite handling of sodium and water excretion. For example, an acute deficit in ECF volume (i.e., hypovolemia) elicits an increase in VP release to promote water retention (Robertson et al., 1976), but this response is accompanied by a decrease in natriuresis to ensure that the fluid being accumulated remains isotonic (Bennett and Gardiner, 1986). Increases in VP secretion during mild hypovolemia are specifically associated with an increase in the slope of the proportional relation between plasma [VP] and osmolality (Robertson et al., 1976). However, OT secretion is negligible under such conditions (Koehler et al., 1994; Stricker et al., 1994), thus minimizing natriuresis. An animal's state of volemia can therefore cause antiparallel changes in the osmoregulation of VP and OT release to optimize the central control of fluid homeostasis. Specifically, hypovolemia may inhibit the excitatory effect of hypertonicity on OT neurons, while potentiating its excitatory effect on VP neurons.

State-dependent switching from parallel to antiparallel control of VP and OT neurons during hypovolemia could be achieved by release of a neuromodulator that induces opposite changes in the efficacy of OVLT → SON_{OT} and OVLT → SON_{VP} transmission. Previous studies have shown that the neuropeptide angiotensin II (Ang II) serves as a multifunctional mediator of coordinated peripheral and central homeostatic responses during hypovolemia (Antunes-Rodrigues et al., 2004). Ang II is found in many parts of the brain and is enriched in subfornical organ neurons that project to the SON (Jhamandas et al., 1989). Experiments in vivo have shown that subfornical organ neurons become excited during hypovolemia (Potts et al., 2000), indicating that release of Ang II into the SON could serve as a local

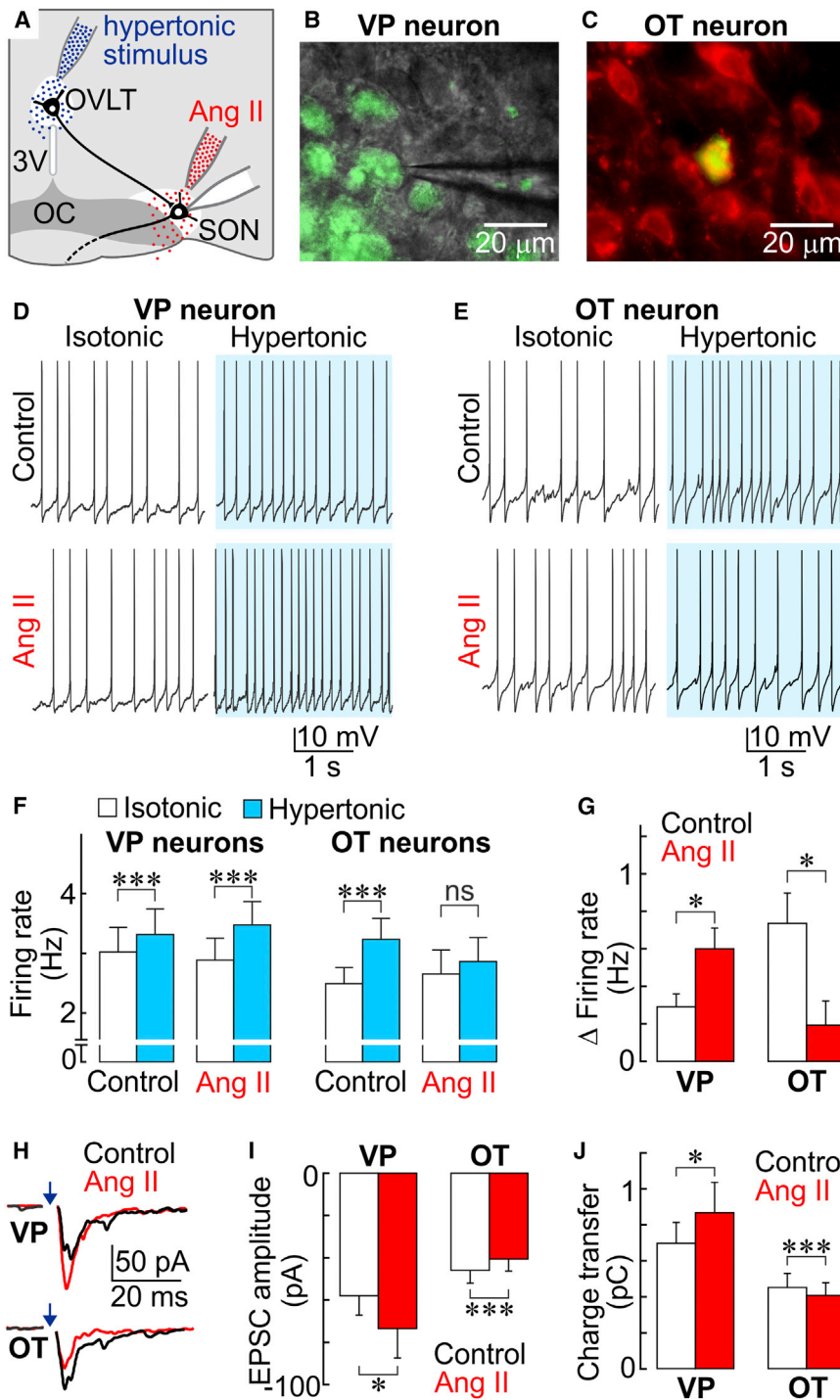


Figure 1. Ang II Causes Antiparallel Changes in Osmotic Excitation of VP and OT Neurons

(A) Schematic diagram of the experimental setup used to record from rat SON neurons in angled hypothalamic slices (3V, third ventricle; OC, optic chiasma). All experiments performed in the presence of 100 μ M picrotoxin to block GABA transmission.

(B) VP neuron expressing enhanced green fluorescent protein.

(C) Neuron (yellow) identified as OT positive by post hoc detection of neurobiotin injected during the recording and immunolabeling (red) with OT antibodies.

(D and E) Voltage traces show action potential firing in the absence (control) and presence of Ang II, both before (isotonic) and during application of a hypertonic stimulus to the OVLT (blue shading). The excitatory effect of hypertonicity depends on glutamatergic synapses (Figure S1).

(F) Bar graphs plot mean (\pm SEM) firing rates observed in VP and OT neurons before (isotonic) and during the application of a hypertonic stimulus to the OVLT (blue bars), both in control conditions or while Ang II was applied within the SON. Note that baseline (isotonic) firing was adjusted before each trial. See Figure S2 and Supplemental Information. *** $p < 0.001$; ns, not significant.

(G) Bars plot mean (\pm SEM) changes in firing rate (Δ Firing rate) induced by hypertonic stimulation of the OVLT in VP and OT neurons exposed to Ang II (red bars) or under control conditions (* $p < 0.05$).

(H) EPSCs evoked by electrical stimuli (arrows) delivered to the OVLT (each sweep is an average of ten consecutive trials) in the absence and presence of Ang II, in VP and OT neurons.

(I and J) Bar graphs plot the effects of Ang II on mean (\pm SEM) EPSC amplitude (I) or charge transfer (J) in VP and OT neurons. * $p < 0.05$; *** $p < 0.001$. See also Figure S3.

molecular indicator of hypovolemia. Recent studies have shown that activation of metabotropic receptors on SON neurons can lead to the production of retrograde messengers that can bidirectionally modulate synaptic transmission in a cell-type- (Zampronio et al., 2010) and synapse-specific fashion (Di et al., 2009). In this study, we tested the hypothesis that Ang II can induce antiparallel changes in osmotic control of VP and OT

neurons by inducing opposite changes on the strength of synaptic signaling in OVLT \rightarrow SON_{OT} and OVLT \rightarrow SON_{VP}. we obtained whole-cell patch-clamp recordings from identified SON neurons in angled slices of adult rat hypothalamus, which maintain OVLT \rightarrow SON connectivity (Figure 1A). In agreement with previous studies (Richard and Bourque, 1995; Trudel and Bourque, 2010), brief (30–60 s) application of hypertonic saline (+20 mM mannitol) to the OVLT significantly increased action potential firing rate in MNCs relative to baseline and this effect

neurons by inducing opposite changes on the strength of synaptic signaling in OVLT \rightarrow SON_{OT} and OVLT \rightarrow SON_{VP}.

RESULTS

Ang II Induces Opposite Changes in Osmotic Signaling to VP and OT Neurons

To determine if Ang II has an opposite effect on VP and OT neurons during hyperosmotic stimulation of the OVLT,

was abolished by bath application of kynurenic acid (3 mM) to block ionotropic glutamate receptors (Figure S1).

Recording from identified MNCs (Figures 1B and 1C) confirmed that hypertonic stimulation of the OVLT increases firing rate of both VP (from 3.02 ± 0.41 Hz to 3.31 ± 0.43 Hz; $p = 0.00076$; $n = 17$) and OT neurons (from 2.49 ± 0.27 to 3.23 ± 0.35 Hz; $p = 0.00076$; $n = 12$; Figures 1D–F). Ang II was then applied locally within the SON (10^{-5} M; delivered >60 s before and during each test). After eliminating the postsynaptic excitatory effect of Ang II (Chakfe and Bourque, 2000) with hyperpolarizing current (<10 pA), the effect of the hyperosmotic stimulus was re-examined (Figures 1D–1G). VP neurons were still excited by hypertonicity in the presence of Ang II (from 2.88 ± 0.37 Hz to 3.47 ± 0.39 Hz; $p = 0.000045$; $n = 17$); however, the average change in firing rate induced by hypertonicity was significantly greater in the presence of the peptide ($+0.60 \pm 0.11$ Hz in Ang II versus $+0.29 \pm 0.07$ Hz without Ang II; $p = 0.019$; $n = 17$; Figures 1G and S2). Conversely, application of Ang II into the SON inhibited the excitatory effect of hyperosmotic stimulation of the OVLT on OT neurons (from 2.67 ± 0.40 Hz to 2.87 ± 0.40 Hz; $p = 0.154$; $n = 12$; Figures 1F and 1G). Ang II therefore potentiates the excitation of VP neurons caused by physiological activation of osmosensory afferents but suppresses the response of OT neurons to the same stimulus.

To determine if this antiparallel effect of Ang II was associated with cell-type-specific changes in synaptic transmission, we examined the effect of the peptide on excitatory postsynaptic currents (EPSCs) evoked by electrical stimulation the OVLT. Local application of Ang II into the SON (4 min) caused a significant and reversible increase of EPSC amplitude in VP cells (from -58.1 ± 9.2 to -73.6 ± 13.9 pA; $p = 0.02$; $n = 12$; Figures 1H, 1I, and S3). In contrast, OT neurons showed a significant reduction in EPSC amplitude in the presence of Ang II (from -46.1 ± 6.1 to -40.8 ± 5.7 pA; $p = 0.0002$; $n = 19$; Figures 1H and 1I). Because EPSCs observed in MNCs are followed by an important proportion of asynchronous events (Iremonger and Bains, 2007), we also quantified the effects of Ang II on synaptically induced charge transfer (ΔQ). Similar to its effects on peak EPSC amplitude, Ang II caused a significant increase of ΔQ in VP neurons (from -0.698 ± 0.116 pC to -0.868 ± 0.168 pC; $p = 0.03$; $n = 12$) and reduced ΔQ in OT neurons (from -0.452 ± 0.078 pC to -0.408 ± 0.070 pC; $p = 0.0008$; $n = 19$; Figure 1J). Changes in electrically evoked synaptic transmission caused by Ang II were sustained during application lasting as long as 10 min (data not shown) and were accompanied by significant increases in the amplitude and frequency of spontaneous EPSCs (sEPSCs) recorded in VP neurons and by the reverse effect in OT neurons (Figure S4).

Ang II Has Opposite Effects on Presynaptic Glutamate Release onto OT and VP Neurons

Presynaptic changes in Ca^{2+} -dependent neurotransmitter release probability (P_R) are commonly associated with inverse changes in short-term facilitation (Dobrunz and Stevens, 1997). We therefore examined if changes in excitatory transmission caused by Ang II were associated with changes in paired pulse facilitation. For this purpose pairs of electrical stimuli applied 60 ms apart were delivered to the OVLT, and the paired pulse

ratio (PPR) was calculated from the amplitudes of the evoked EPSCs (i.e., $\text{PPR} = \text{EPSC}_2/\text{EPSC}_1$) or from the amounts of ΔQ elicited by the consecutive pulses (i.e., $\text{PPR} = \Delta Q_2/\Delta Q_1$). Local application of Ang II had opposite effects on PPR in OT and VP neurons. Specifically, Ang II significantly reduced PPR in VP neurons, regardless of whether it was calculated from EPSC amplitudes (from 2.63 ± 0.17 to 1.98 ± 0.14 ; $p = 0.0001$; $n = 12$; Figure 2A) or from differences in ΔQ (from 2.77 ± 0.22 to 2.15 ± 0.14 ; $p = 0.001$; $n = 12$). Conversely, Ang II significantly increased PPR in OT neurons, whether calculated from EPSC amplitudes (from 2.04 ± 0.15 to 2.49 ± 0.24 ; $p = 0.002$; $n = 19$; Figure 2B) or from values of ΔQ (from 2.05 ± 0.17 to 2.43 ± 0.18 ; $p = 0.02$; $n = 19$).

Changes in P_R are also associated with inversely proportional changes in the frequency at which synaptic failures are observed during a series of trials performed with low intensity stimulation (Dobrunz and Stevens, 1997). As illustrated in Figure 2C, Ang II significantly reduced the rate of synaptic failures observed in VP neurons (from $38.5\% \pm 5.0\%$ to $32.2\% \pm 4.5\%$; $p = 0.04$; $n = 15$). Conversely, the incidence of failures was significantly increased in OT neurons (from $33.0\% \pm 5.7\%$ to $40.9\% \pm 6.9\%$; $n = 14$; $p = 0.01$; Figure 2D).

Electrically evoked EPSCs in SON neurons are followed by asynchronous EPSCs (aEPSCs) caused by a transient and Ca^{2+} -dependent increase in P_R at stimulated nerve terminals (Iremonger and Bains, 2007). Ang II-mediated changes in P_R should therefore be associated with changes in aEPSC frequency, whereas changes in postsynaptic AMPA receptor density or function should cause changes in aEPSC amplitude (quantal size). We therefore examined the frequency and amplitude of aEPSCs detected during a 100 ms window immediately following the decay of the evoked EPSC in the absence and presence of Ang II. As illustrated in Figure 2E, Ang II caused a significant increase in the mean aEPSC frequency in VP neurons (from 79.9 ± 5.4 Hz to 109.5 ± 5.9 Hz; $n = 7$; $p = 0.008$), whereas it significantly decreased aEPSC frequency in OT neurons (from 103.2 ± 13.7 Hz to 80.8 ± 12.0 Hz; $n = 7$; $p = 0.0186$; Figure 2F). Ang II had no effect on mean (\pm SEM) aEPSC amplitude in either VP (-21.8 ± 4.4 pA versus -21.3 ± 3.9 pA in Ang II; $p = 0.624$; $n = 7$) or OT neurons (-27.1 ± 4.5 pA versus -26.8 ± 4.5 pA in Ang II; $p = 0.765$; $n = 7$). The effects of Ang II on OVLT \rightarrow SON synapses are therefore mediated through changes in P_R , and increases in sEPSC amplitude are likely caused by increases in the quantal content of a proportion of network-dependent synaptic events.

To determine if changes in synaptic strength are sufficient to modulate spike output, we applied simulated synaptic activity as a dynamic current clamp command in naive SON neurons in the presence of 20 μM DNQX and 100 μM picrotoxin. Dynamic command templates constructed from native synaptic activity previously recorded in VP and OT neurons featured 10 s of baseline activity, followed by 10 s of potentiated or weakened sEPSC activity (Figure 3A). Cells exposed to the weakening synaptic template displayed a significant decrease in spike output (from 1.3 ± 0.2 Hz to 1.1 ± 0.3 Hz; $p = 0.0479$; $n = 15$; Figures 3A and 3B), whereas those exposed to the potentiating template displayed a significant increase in spike output (from 1.1 ± 0.2 Hz to 1.3 ± 0.2 Hz; $p = 0.0123$; $n = 15$; Figures 3A and 3C).

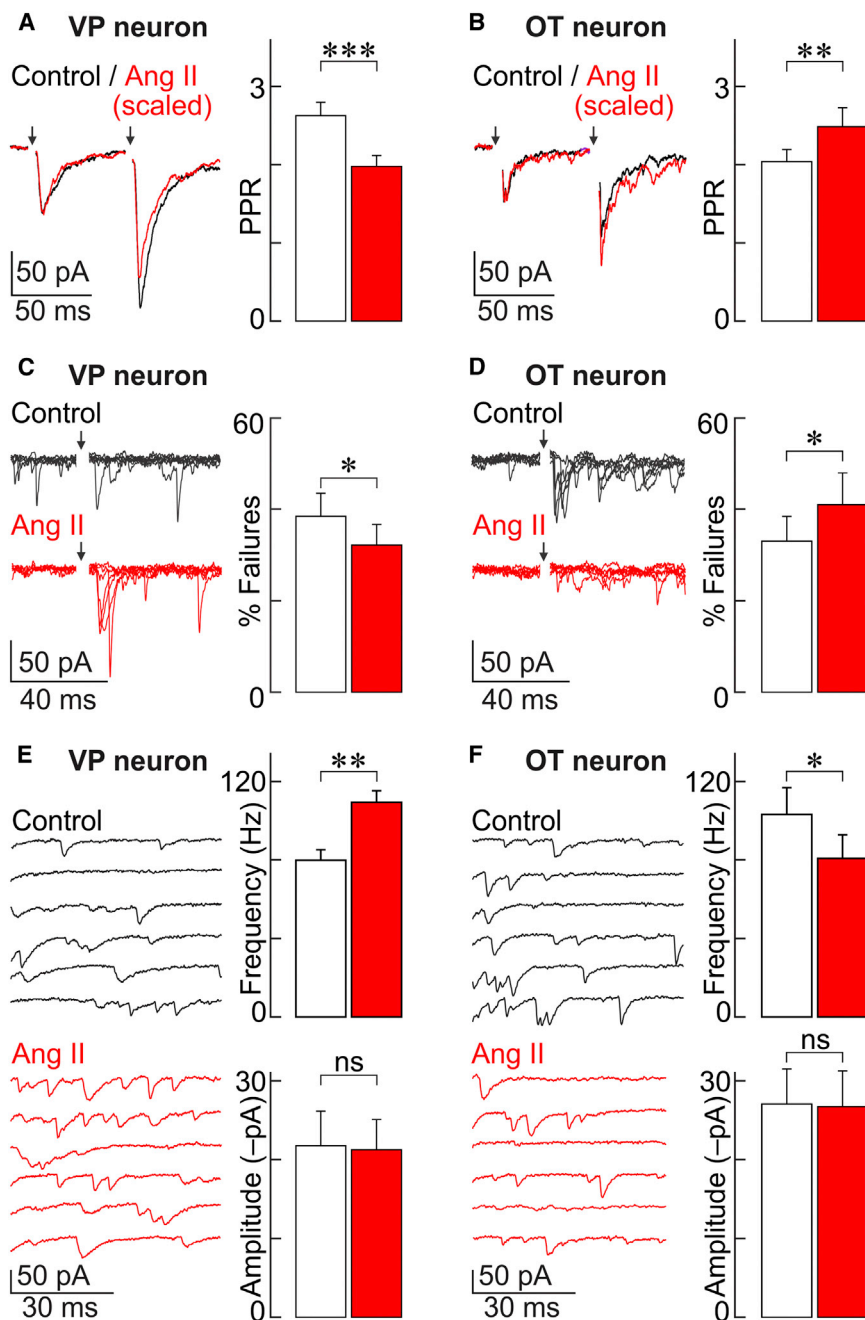


Figure 2. Ang II Modulates Presynaptic Release Probability

(A and B) traces show EPSCs (average of ten sweeps) evoked by pairs of stimuli (60 ms apart) delivered to the OVLT (arrows) in VP (A) and OT neurons (B) in the absence and presence of Ang II. Traces in Ang II (red) are scaled so amplitudes of EPSC₁ are equal in the two conditions. Bar graphs in each panel plot mean (±SEM) values of PPR in the two conditions (**p < 0.01; ***p < 0.001).

(C and D) Traces on the left show six consecutive superimposed sweeps where a single minimal stimulus was delivered to the OVLT (arrow). Note that Ang II reduces failures in the VP neuron (C) but increases failure rate in the OT neuron (D). Bar graphs in each panel plot the mean (±SEM) percentage of sweeps showing failures in the various conditions. *p < 0.05.

(E and F) Left panels show aEPSCs recorded after the decay of OVLT-evoked EPSCs (data not shown) in the absence (Control, six sweeps) and presence of Ang II (six red sweeps). Bar graphs on the right show the effects of Ang II (red bars) on mean (±SEM) aEPSC frequency and amplitude compared to control (white bars) in VP (E) and OT neurons (F). **p < 0.01; *p < 0.05; ns, not significant.

mimic the effects of Ang II on evoked EPSCs. Indeed, EPSC amplitude increased from -50.9 ± 7.2 pA to -57.5 ± 7.9 pA ($p = 0.002$, $n = 8$) and ΔQ increased from 0.807 ± 0.130 pC to 0.901 ± 0.157 pC ($p = 0.02$; $n = 8$). To determine if NO production contributes to the Ang II-mediated facilitation of glutamate synapses on VP neurons, we examined the effects of the NO synthase inhibitor L-NAME. Bath application of L-NAME (10 μ M) prevented the Ang II-evoked increase in EPSC amplitude (control -57.0 ± 12.3 pA versus -55.8 ± 10.8 pA in Ang II, $p = 0.3$; $n = 10$; Figure 4A) and ΔQ (control 0.672 ± 0.121 pC versus 0.669 ± 0.106 pC in Ang II; $p = 0.4$; $n = 10$), as well as associated changes in PPR determined from EPSC amplitudes (from 1.89 ± 0.20 to 1.80 ± 0.12 ; $p = 0.3$; $n = 10$) or ΔQ (from 1.94 ± 0.18

Ang II Triggers Cell-Type-Specific and Cell-Autonomous Retrograde Signaling

SON neurons express nitric oxide (NO) synthase (Bredt et al., 1990), which is localized to synaptic junctions through an interaction with PSD-95 (Brenman et al., 1996). Experiments in vivo and in vitro indicate that NO facilitates release of glutamate and GABA in the SON through presynaptic activation of soluble guanylyl cyclase (Engelmann et al., 2002; Gillard et al., 2007; Vacher et al., 2003). In agreement, we found that bath application of the NO donor sodium nitroprusside (SNP, 10^{-7} M) could

to 1.85 ± 0.12 ; $p = 0.2$; $n = 10$). Ang II-evoked facilitation of EPSC amplitude was also prevented when 1 μ M L-NAME was applied only to the postsynaptic cell via the recording pipette (-86.1 ± 24.6 pA versus -87.7 ± 23.4 pA in Ang II; $p = 0.4$; $n = 6$; data not shown).

Previous work has shown that the endocannabinoids (eCBs) anandamide and 2-arachidonoyl glycerol can be released in the SON (Di et al., 2005a), and activation of cannabinoid type 1 (CB1) receptors has been found to inhibit glutamate release in this nucleus both in vivo (Sabatier and Leng, 2006)

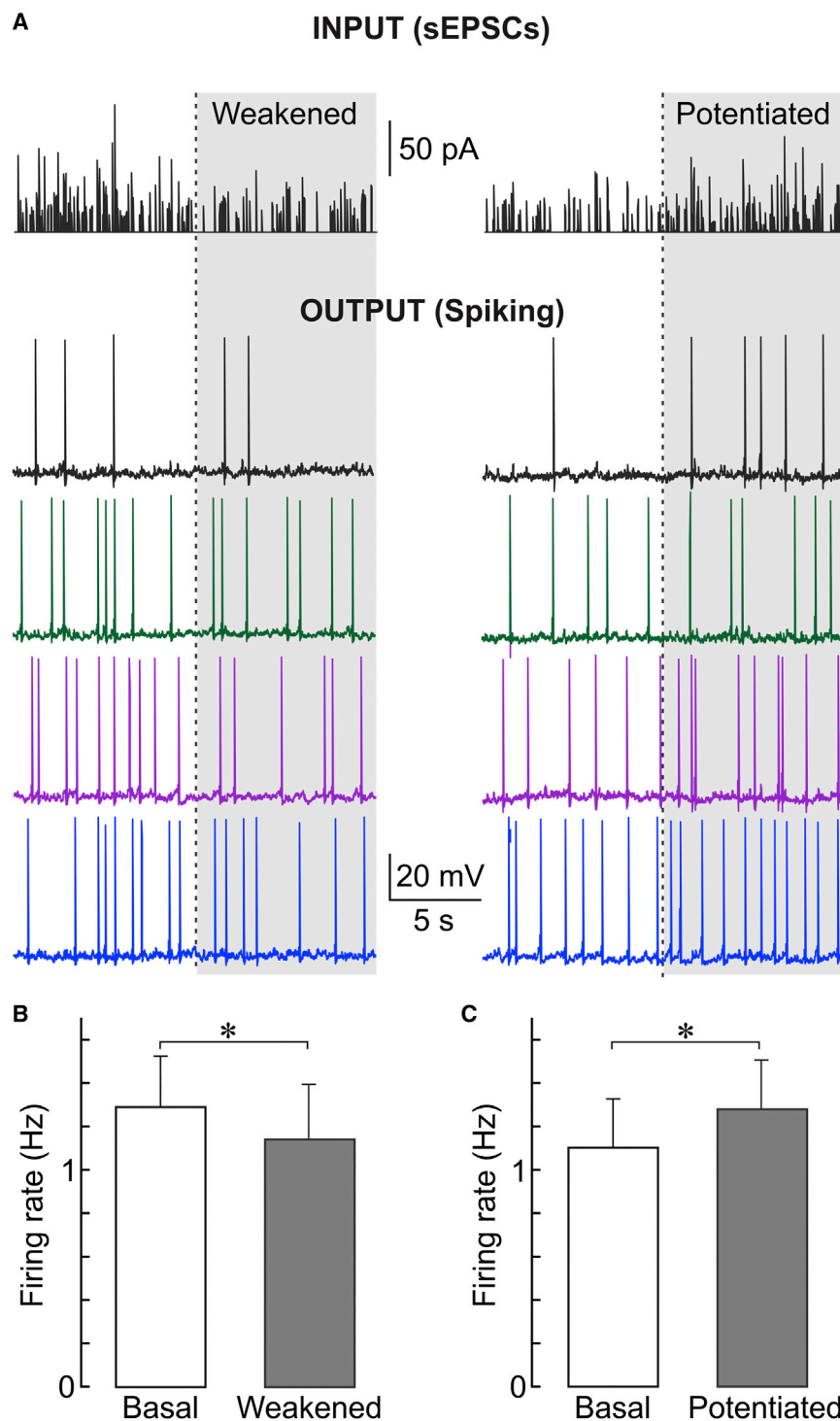


Figure 3. Changes in Synaptic Strength Are Sufficient to Modulate Spike Output

(A) Upper traces show dynamic synaptic command templates featuring transitions from basal to weakened (left, shaded area), or from basal to potentiated synaptic activity (right, shaded area; see Figure S4). Basal firing activity recorded in the presence of DNQX and bicuculline was adjusted to a near threshold level prior to each test. Lower traces show the voltage responses of four different cells to the template commands.

(B and C) Bar graphs plot the mean (\pm SEM) firing rates observed in the group of cells tested ($n = 15$; * $p < 0.05$).

0.423 ± 0.078 pC versus 0.419 ± 0.087 pC in Ang II; $p = 0.4$; $n = 12$), and changes in PPR determined from amplitudes (from 1.95 ± 0.21 to 2.08 ± 0.19 ; $p = 0.3$; $n = 12$) or ΔQ (from 2.01 ± 0.18 to 2.23 ± 0.18 ; $p = 0.1$; $n = 12$). Note that antagonism of NO production had no effect on Ang II-evoked synaptic depression in OT cells, and CB1 receptor antagonism had no effect on Ang II-evoked facilitation in VP cells (Figure 4A).

Blockade of Ang II-mediated facilitation by application of L-NAME via the recording pipette indicates that NO production by a single VP neuron is sufficient to mediate local retrograde signaling. To confirm this result and determine if the Ang II-mediated suppression of EPSCs is also a cell-autonomous process, we examined the effect of including GDP- β -S (10^{-6} M) in the patch pipette to prevent activation of G protein signaling cascades in the cell being recorded. In VP neurons loaded with GDP- β -S, Ang II failed to enhance EPSC amplitude (control -33.0 ± 5.0 pA versus -32.6 ± 4.8 pA in Ang II; $p = 0.4$; $n = 9$; Figure 4A) or ΔQ (control 0.539 ± 0.147 pC versus 0.556 ± 0.157 pC in Ang II; $p = 0.2$; $n = 9$). Analogously, the inhibitory effects of Ang II on EPSCs were inhibited in OT neurons filled with GDP- β -S (amplitude was -49.0 ± 8.7 pA in control versus -48.6 ± 7.3 pA in Ang II, $p =$

and in vitro (Di et al., 2005a). We therefore examined if CB1 receptors are involved in the Ang II-induced suppression of EPSCs in OT cells. Application of the CB1 receptor antagonist AM251 ($0.5 \mu\text{M}$) fully prevented the inhibitory effect of Ang II on OVLT-mediated EPSC amplitude (control -38.5 ± 5.4 pA versus -37.1 ± 4.6 pA in Ang II; $p = 0.3$; $n = 12$) and ΔQ (control

0.4 , and ΔQ was 0.581 ± 0.156 pC in control versus 0.545 ± 0.114 pC in Ang II; $p = 0.3$; $n = 9$; Figure 4A). These findings indicate that a cell-autonomous production of NO and eCBs underlies the Ang II-mediated retrograde facilitation and inhibition of presynaptic glutamate release onto VP and OT neurons, respectively (Figure 4B).

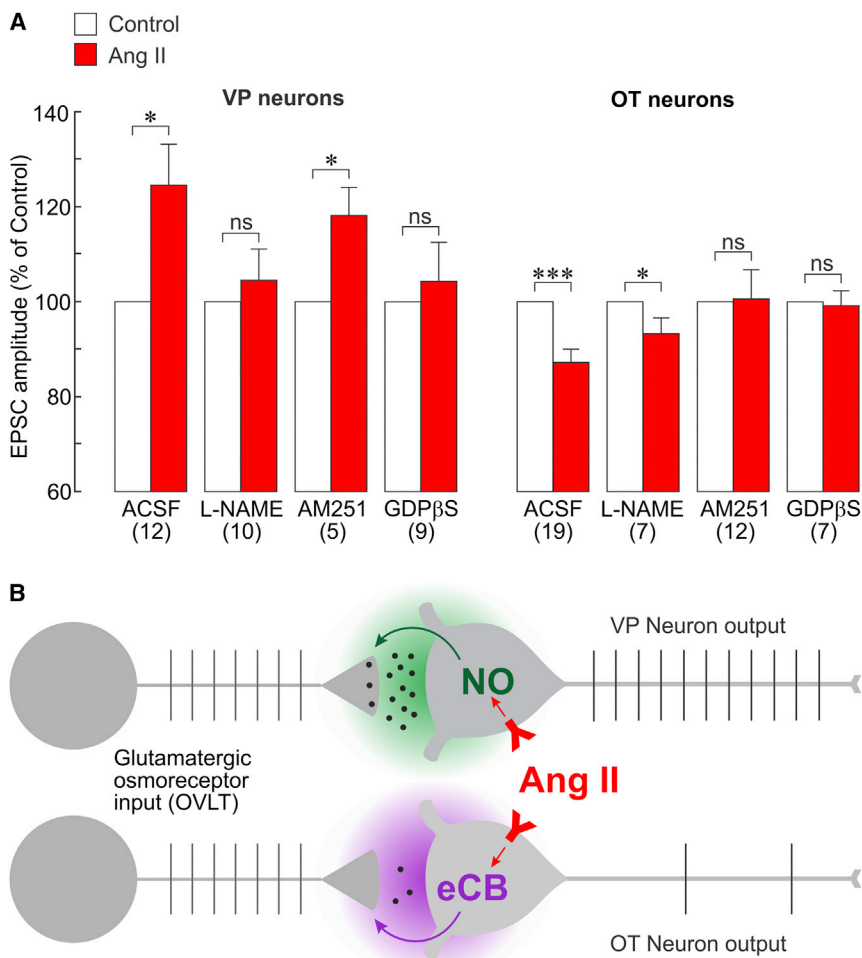


Figure 4. Ang II Alters Synaptic Transmission via Cell-Autonomous Release of Different Retrograde Signals

(A) Bar graphs plot mean (\pm SEM) normalized changes in evoked EPSC amplitude caused by Ang II (red bars) in VP (left) and OT neurons (right) under different conditions. The effects of Ang II in each condition are expressed relative to the amplitude of EPSCs recorded in the same cell in the absence of Ang II (ACSF, white bars; * $p < 0.05$; *** $p < 0.001$; ns, not significant).

(B) Schematic diagram illustrating our conclusion that cell-autonomous production of NO mediates the increase in glutamate release and enhanced synaptic excitation of VP neurons caused by Ang II, whereas endocannabinoid (eCB) production mediates reduced glutamate release and attenuated synaptic excitation in OT neurons. Note that our data do not exclude the possibility that Ang II receptors are located elsewhere.

uretic VP release as a result of increased osmotic responsiveness (Robertson et al., 1976). Although the osmotic regulation of OT secretion normally parallels that of VP (Bourque, 2008), stimulation of salt-wasting OT secretion is prevented during moderate hypovolemia (Koehler et al., 1994; Stricker et al., 1994). Thus, the divergent requirements for VP and OT responsiveness under these conditions predict an antiparallel modulation of osmoreceptor inputs to VP and OT neurons.

Previous work has shown that neuropeptides can regulate central osmoregulatory circuits in a cell-type-specific manner. For instance, alpha melanocyte stimulating hormone can selectively inhibit excitatory synapses contacting OT-releasing neurons but not those on VP MNCs (Sabatier and Leng, 2006). In contrast, endothelin has been shown to inhibit unidentified excitatory synapses on VP neurons and facilitate those on OT neurons (Zampronio et al., 2010). Our results now reveal that Ang II can act as a cell-type-specific switch to differentially regulate the efficacy of the OVLT \rightarrow SON_{OT} and OVLT \rightarrow SON_{VP} pathways. In VP cells, Ang II facilitates spiking induced by osmotic activation of OVLT afferents, whereas that of OT cells is suppressed, matching changes in VP and OT secretion observed during moderate hypovolemia in vivo (Koehler et al., 1994; Stricker et al., 1994).

Although our findings indicate that the effects of Ang II on synaptic transmission are specifically mediated by changes in presynaptic P_R, previous work has shown that Ang II can also modulate postsynaptic ion channels and alter the excitability of MNCs (Chakfe and Bourque, 2000; Nagatomo et al., 1995). However, these studies did not report opposite actions of Ang II on OT- and VP-releasing neurons, making it unlikely that such effects could account for an antiparallel modulation of the OVLT's influence on OT and VP MNCs. Indeed, we found that the spiking output of MNCs can be significantly

DISCUSSION

Ang II Is a State-Dependent Circuit Switch

Principles of neuromodulation are conserved across invertebrate and vertebrate species, such as the ability of neuropeptides to globally coordinate the activity of diverse networks to evoke defined behavioral patterns (Garrison et al., 2012) or to gate the transmission of sensory information. For example, in *Drosophila* and *C. elegans*, neuropeptide F and octopamine are respectively used to provoke context-dependent changes in responsiveness to sensory cues that adapt foraging behavior to hunger state (Bargmann, 2012). Experiments in mammals have shown that ghrelin and leptin can induce opposing changes in synaptic strength that flip hypothalamic circuits between two stable activity levels according to physiological state (Yang et al., 2011). Using these principles of circuit modulation and sensory gating, neuropeptides can direct circuits and behavior toward meeting a physiological need.

Recovery from acute hypovolemia (e.g., following hemorrhage) requires the retention of both water and sodium to promote an accumulation of isotonic fluid (Antunes-Rodrigues et al., 2004). Moderate hypovolemic states (<20% blood volume depletion) are associated with a noticeable increase in antidi-

altered by changes in sEPSCs alone (Figure 3), indicating that the presynaptic actions of Ang II are sufficient to provide an efficient modulation of cell-type and circuit-specific network activity.

Cell-Type Specificity Reflects Cell-Autonomous Retrograde Signaling

The cell-autonomous effects of Ang II on osmoreceptor inputs were mediated by losartan-sensitive AT₁ receptors in both OT and VP neurons (data not shown). Thus, cell-type specificity likely results from the activation of distinct complements of effector G proteins that drive production of different retrograde messengers in OT and VP neurons. Indeed, previous work has shown that glucocorticoid activation of G_{αs} can trigger cAMP-dependent release of eCBs to suppress excitatory synaptic transmission, whereas release of the G_{βγ} subunit leads to NO production to enhance inhibitory synaptic transmission (Di et al., 2009). The signaling mechanisms responsible for the differential production of eCBs and NO in Ang II-stimulated OT and VP neurons remain to be established.

Although eCBs and NO can readily diffuse from their site of production to their presynaptic site of action, previous studies have shown that the effects of these retrograde messengers can be spatially constrained to single cells or subsets of synapses (Di et al., 2005b; Hall and Garthwaite, 2009; Wilson and Nicoll, 2002). Indeed, our observation that the effects of Ang II can be prevented by blocking G protein signaling in a single target cell indicates that the cell-type-specific production of eCBs or NO is sufficiently constrained spatially to mediate an antiparallel modulation of adjacent excitatory synapses in the OVLV → SON_{VP} and OVLV → SON_{OT} pathways. Thus neuropeptide activation of cell-type-specific retrograde signals can mediate a state-dependent circuit switch that adapts network activity to a desired physiological outcome.

EXPERIMENTAL PROCEDURES

Animals

Experiments were performed on male Long-Evans rats (50–80 g, Charles River Laboratories) or transgenic VPeGFP male and female Wistar rats (50–250 g) anesthetized with halothane and sacrificed in accordance with a protocol approved by the McGill University Animal Care Committee. Preparation of angled horizontal hypothalamic slices, immunohistochemical identification, and whole-cell voltage clamp recordings were performed as previously described (Stachniak et al., 2012). See Supplemental Experimental Procedures.

Recording

Glass pipettes (1.2 mm outside diameter, 0.68 mm inside diameter, A-M Systems) were prepared using a P-87 horizontal puller (Sutter Instrument) and filled with an internal solution containing (in mM): K gluconate, 110; MgCl₂, 1; KCl, 10; HEPES 10 and adjusted to pH 7.4 with KOH, 282 milliosmoles/kg with mannitol. For current clamp recordings, the internal solution contained KMeSO₄ instead of K gluconate and 4 mM ATP, 1 mM GTP. Internal solutions with N^G-nitro-L-arginine methyl ester hydrochloride (L-NAME, 1 μM, Sigma-Aldrich) or GDP-β-S (a nonhydrolyzable form of guanosine diphosphate, 1 μM, Sigma) were used where indicated. Pipette resistance was 2–4 MΩ. In some cases, neurobiotin (Vector Laboratories, 0.2% w/v) was added to the pipette. Pipette series resistance as 5–15 MΩ. Whole-cell current and voltage was recorded using an Axopatch-1D amplifier (Axon Instruments), displayed on an oscilloscope and digitized using pCLAMP 8.0 software

(2–20 kHz). AM-251 (Tocris Bioscience, final concentration 0.5 μM) was dissolved 1:10,000 in DMSO. See Supplemental Experimental Procedures.

Synaptic Template Commands

Dynamic command templates were constructed from 10 s segments of native sEPSCs recorded under normal and Ang II modulated conditions (1–1,200 Hz band-pass filtered, noise between events removed). Consecutive segments were arranged to produce transitions between basal and potentiated (from 1.61 to 4.48 pC total ΔQ), or basal and weakened synaptic activity (from 6.25 to 2.60 pC total ΔQ). The sEPSC samples chosen to construct the templates corresponded to the upper range of changes in sEPSC-mediated ΔQ induced by Ang II in VP and OT neurons. The impact of the templates on spike output was determined by comparing mean firing rates observed during consecutive segments. Cells were excluded from the analysis if resistance was less than 200 MΩ or if basal firing rate was not stable.

Immunohistochemistry

After recording, slices were fixed in phosphate buffered saline (PBS) containing 4% paraformaldehyde for 2 days, then washed in PBS and blocked at room temperature (PBS, 1% normal goat serum and 0.3% Triton X-100; 1 hr). Slices were incubated for 1–4 days at 4°C with primary antibodies (provided by Hal Gainer), incubated in labeled secondary (Invitrogen) for 2 hr, and washed in PBS. See Supplemental Experimental Procedures.

Statistics

All values are reported as mean ± SEM. Statistical tests performed using Sigmaplot 12 (Systat Software) included Student's t test or paired t test, as appropriate. Differences between cumulative event distributions (Figure S5) were compared using the Kolmogorov-Smirnov test (Clampfit 10.0). A p value <0.05 was considered statistically significant.

SUPPLEMENTAL INFORMATION

Supplemental Information includes Supplemental Experimental Procedures and four figures and can be found with this article online at <http://dx.doi.org/10.1016/j.celrep.2014.06.029>.

ACKNOWLEDGMENTS

This work was supported by a James McGill Chair and by Canadian Institutes of Health Research (CIHR) operating grants MOP9939 and FRN82818 to C.W.B. T.J.S. was supported by Doctoral Awards from CIHR and the Heart and Stroke Foundation (HSF) of Canada. The authors gratefully acknowledge Dr. Harold Gainer for supplying antibodies and Dr. Yoichi Ueta for providing VP-eGFP transgenic rats.

Received: June 21, 2013

Revised: May 24, 2014

Accepted: June 18, 2014

Published: July 17, 2014

REFERENCES

- Antunes-Rodrigues, J., de Castro, M., Elias, L.L., Valença, M.M., and McCann, S.M. (2004). Neuroendocrine control of body fluid metabolism. *Physiol. Rev.* 84, 169–208.
- Bargmann, C.I. (2012). Beyond the connectome: how neuromodulators shape neural circuits. *BioEssays* 34, 458–465.
- Bennett, T., and Gardiner, S.M. (1986). Fluid and electrolyte handling in Long Evans and Brattleboro rats following injection of polyethylene glycol. *J. Physiol.* 381, 407–415.
- Bourque, C.W. (2008). Central mechanisms of osmosensation and systemic osmoregulation. *Nat. Rev. Neurosci.* 9, 519–531.
- Bredt, D.S., Hwang, P.M., and Snyder, S.H. (1990). Localization of nitric oxide synthase indicating a neural role for nitric oxide. *Nature* 347, 768–770.

- Brenman, J.E., Chao, D.S., Gee, S.H., McGee, A.W., Craven, S.E., Santillano, D.R., Wu, Z., Huang, F., Xia, H., Peters, M.F., et al. (1996). Interaction of nitric oxide synthase with the postsynaptic density protein PSD-95 and alpha1-syntrophin mediated by PDZ domains. *Cell* 84, 757–767.
- Chakfe, Y., and Bourque, C.W. (2000). Excitatory peptides and osmotic pressure modulate mechanosensitive cation channels in concert. *Nat. Neurosci.* 3, 572–579.
- Ciura, S., and Bourque, C.W. (2006). Transient receptor potential vanilloid 1 is required for intrinsic osmoreception in organum vasculosum lamina terminalis neurons and for normal thirst responses to systemic hyperosmolality. *J. Neurosci.* 26, 9069–9075.
- Di, S., Boudaba, C., Popescu, I.R., Weng, F.J., Harris, C., Marcheselli, V.L., Bazan, N.G., and Tasker, J.G. (2005a). Activity-dependent release and actions of endocannabinoids in the rat hypothalamic supraoptic nucleus. *J. Physiol.* 569, 751–760.
- Di, S., Malcher-Lopes, R., Marcheselli, V.L., Bazan, N.G., and Tasker, J.G. (2005b). Rapid glucocorticoid-mediated endocannabinoid release and opposing regulation of glutamate and gamma-aminobutyric acid inputs to hypothalamic magnocellular neurons. *Endocrinology* 146, 4292–4301.
- Di, S., Maxson, M.M., Franco, A., and Tasker, J.G. (2009). Glucocorticoids regulate glutamate and GABA synapse-specific retrograde transmission via divergent nongenomic signaling pathways. *J. Neurosci.* 29, 393–401.
- Dobrunz, L.E., and Stevens, C.F. (1997). Heterogeneity of release probability, facilitation, and depletion at central synapses. *Neuron* 18, 995–1008.
- Engelmann, M., Wolf, G., and Horn, T.F. (2002). Release patterns of excitatory and inhibitory amino acids within the hypothalamic supraoptic nucleus in response to direct nitric oxide administration during forced swimming in rats. *Neurosci. Lett.* 324, 252–254.
- Garrison, J.L., Macosko, E.Z., Bernstein, S., Pokala, N., Albrecht, D.R., and Bargmann, C.I. (2012). Oxytocin/vasopressin-related peptides have an ancient role in reproductive behavior. *Science* 338, 540–543.
- Gillard, E.R., Coburn, C.G., de Leon, A., Snissarenko, E.P., Bauce, L.G., Pittman, Q.J., Hou, B., and Currás-Collazo, M.C. (2007). Vasopressin auto-receptors and nitric oxide-dependent glutamate release are required for somatodendritic vasopressin release from rat magnocellular neuroendocrine cells responding to osmotic stimuli. *Endocrinology* 148, 479–489.
- Hall, C.N., and Garthwaite, J. (2009). What is the real physiological NO concentration in vivo? *Nitric Oxide* 21, 92–103.
- Iremonger, K.J., and Bains, J.S. (2007). Integration of asynchronously released quanta prolongs the postsynaptic spike window. *J. Neurosci.* 27, 6684–6691.
- Jhamandas, J.H., Lind, R.W., and Renaud, L.P. (1989). Angiotensin II may mediate excitatory neurotransmission from the subfornical organ to the hypothalamic supraoptic nucleus: an anatomical and electrophysiological study in the rat. *Brain Res.* 487, 52–61.
- Koehler, E.M., McLemore, G.L., Martel, J.K., and Summy-Long, J.Y. (1994). Response of the magnocellular system in rats to hypovolemia and cholecystokinin during pregnancy and lactation. *Am. J. Physiol.* 266, R1327–R1337.
- Nagatomo, T., Inenaga, K., and Yamashita, H. (1995). Transient outward current in adult rat supraoptic neurones with slice patch-clamp technique: inhibition by angiotensin II. *J. Physiol.* 485, 87–96.
- Potts, P.D., Ludbrook, J., Gillman-Gaspari, T.A., Horiuchi, J., and Dampney, R.A. (2000). Activation of brain neurons following central hypervolaemia and hypovolaemia: contribution of baroreceptor and non-baroreceptor inputs. *Neuroscience* 95, 499–511.
- Richard, D., and Bourque, C.W. (1995). Synaptic control of rat supraoptic neurones during osmotic stimulation of the organum vasculosum lamina terminalis in vitro. *J. Physiol.* 489, 567–577.
- Robertson, G.L., Shelton, R.L., and Athar, S. (1976). The osmoregulation of vasopressin. *Kidney Int.* 10, 25–37.
- Sabatier, N., and Leng, G. (2006). Presynaptic actions of endocannabinoids mediate alpha-MSH-induced inhibition of oxytocin cells. *Am. J. Physiol. Regul. Integr. Comp. Physiol.* 290, R577–R584.
- Stachniak, T.J., Sudbury, J.R., Trudel, E., Choe, K.Y., Ciura, S., and Bourque, C.W. (2012). Osmoregulatory circuits in slices and en-bloc preparations of rodent hypothalamus. In *Isolated Central Nervous System Circuits*, K. Balanyi, ed. (New York: Humana-Springer), pp. 211–231.
- Stricker, E.M., Schreihofer, A.M., and Verbalis, J.G. (1994). Sodium deprivation blunts hypovolemia-induced pituitary secretion of vasopressin and oxytocin in rats. *Am. J. Physiol.* 267, R1336–R1341.
- Trudel, E., and Bourque, C.W. (2010). Central clock excites vasopressin neurons by waking osmosensory afferents during late sleep. *Nat. Neurosci.* 13, 467–474.
- Vacher, C.M., Hardin-Pouzet, H., Steinbusch, H.W., Calas, A., and De Vente, J. (2003). The effects of nitric oxide on magnocellular neurons could involve multiple indirect cyclic GMP-dependent pathways. *Eur. J. Neurosci.* 17, 455–466.
- Verbalis, J.G., Mangione, M.P., and Stricker, E.M. (1991). Oxytocin produces natriuresis in rats at physiological plasma concentrations. *Endocrinology* 128, 1317–1322.
- Wilson, R.I., and Nicoll, R.A. (2002). Endocannabinoid signaling in the brain. *Science* 296, 678–682.
- Yang, Y., Atasoy, D., Su, H.H., and Sternson, S.M. (2011). Hunger states switch a flip-flop memory circuit via a synaptic AMPK-dependent positive feedback loop. *Cell* 146, 992–1003.
- Zampronio, A.R., Kuzmiski, J.B., Florence, C.M., Mulligan, S.J., and Pittman, Q.J. (2010). Opposing actions of endothelin-1 on glutamatergic transmission onto vasopressin and oxytocin neurons in the supraoptic nucleus. *J. Neurosci.* 30, 16855–16863.

CELL SPECIFIC RETROGRADE SIGNALS MEDIATE ANTIPARALLEL EFFECTS OF ANGIOTENSIN II ON OSMORECEPTOR AFFERENTS TO VASOPRESSIN AND OXYTOCIN NEURONS

Tevye J. Stachniak, Eric Trudel and Charles W. Bourque

INVENTORY OF SUPPLEMENTAL INFORMATION

SUPPLEMENTAL DATA

- **Figure S1** (Related to Figure 1), shows that the excitatory effects of local hypertonic stimulation of the OVLT on firing in SON neurons depends on glutamatergic synapses.
- **Figure S2** (Related to Figure 1), shows that effects of hypertonicity and Ang II are reproducible.
- **Figure S3** (Related to Figure 1), shows the time course and reversibility of the effects of Ang II on EPSCs evoked by electrical stimulation of the OVLT.
- **Figure S4** (Related to Figure 3), shows changes in sEPSC amplitude and frequency caused by Ang II in OT and VP neurons.

SUPPLEMENTAL EXPERIMENTAL PROCEDURES

- Slice recordings
- Electrical stimulation of the OVLT
- Application of drugs by pressure-ejection
- Identification of OT and VP neurons
- Analysis of firing rates during hypertonic stimulation of the OVLT
- Analysis of evoked EPSCs

SUPPLEMENTARY REFERENCES

Figure S1.

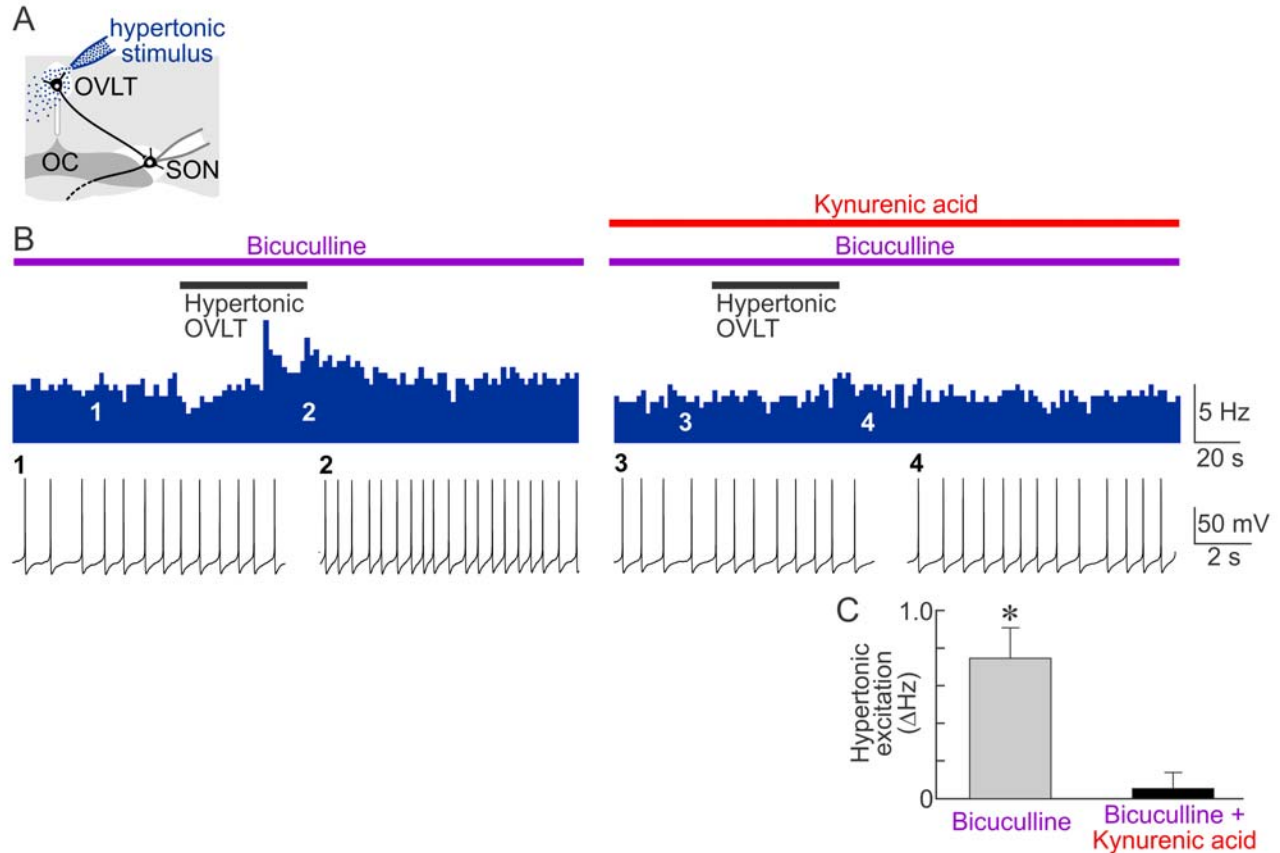


Figure S1 (related to Figure 1). Osmotic activation of MNCs by local hypertonic stimulation of the OVLT requires glutamatergic synapses.

(A) Schematic of the experimental layout. Whole cell recordings are made from MNCs in the supraoptic nucleus (SON) which lies adjacent to the optic chiasma (OC). (B) Blue traces are ratemeter recordings of action potential firing frequency recorded in an MNC (10 μ M bicuculline was present throughout). Application of hypertonic solution to the OVLT (ACSF+20 mM mannitol; black bar) increases firing rate in the absence (left) but not in the presence of 3 mM kynurenic Acid (right). Traces underneath the ratemeter are 3 s voltage excerpts obtained at the times indicated by the numbers. (C) Bar graph shows mean (\pm s.e.m.) changes in firing rate induced by hypertonic stimulation of the OVLT in a group of 5 cells that were tested in the presence of bicuculline alone and in the presence of bicuculline + kynurenic acid (* $p = 0.005$; Paired t -test).

Figure S2

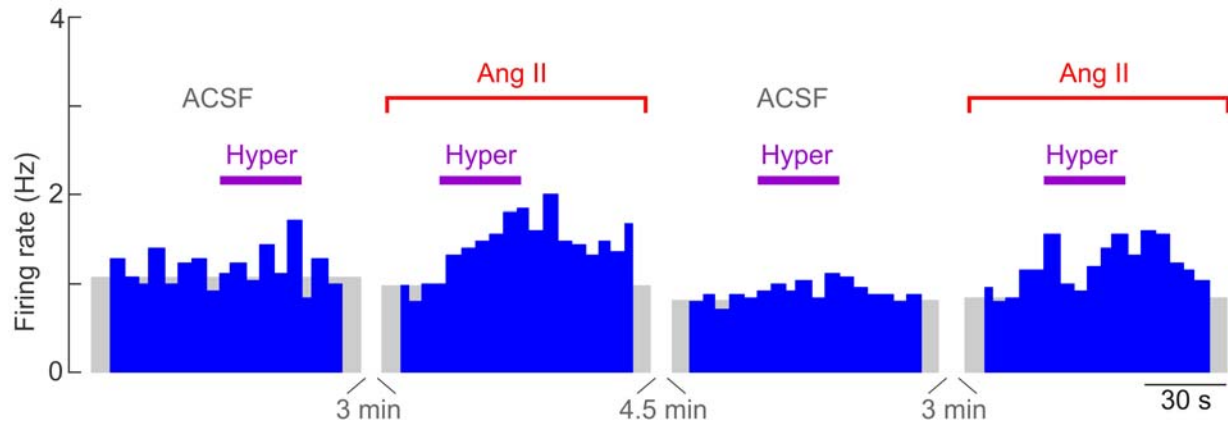


Figure S2 (related to Figure 1). Ang II reproducibly enhances the effects of OVLT hyperosmotic stimulation on MNCs.

Ratemeter plots show action potential firing frequency recorded in a single VP neuron. In each of the 4 trials shown (separated by the time intervals indicated), the baseline firing had been pre-set to a value near 1 Hz by adjusting the holding current (not shown). Holding current was not changed during each of the trials. Note that application of the hyperosmotic solution to the OVLT (Hyper; +20 mosmol/kg; purple bar) consistently causes a slight increase in firing in control conditions (ACSF), but a greater response in the presence of Ang II.

Figure S3

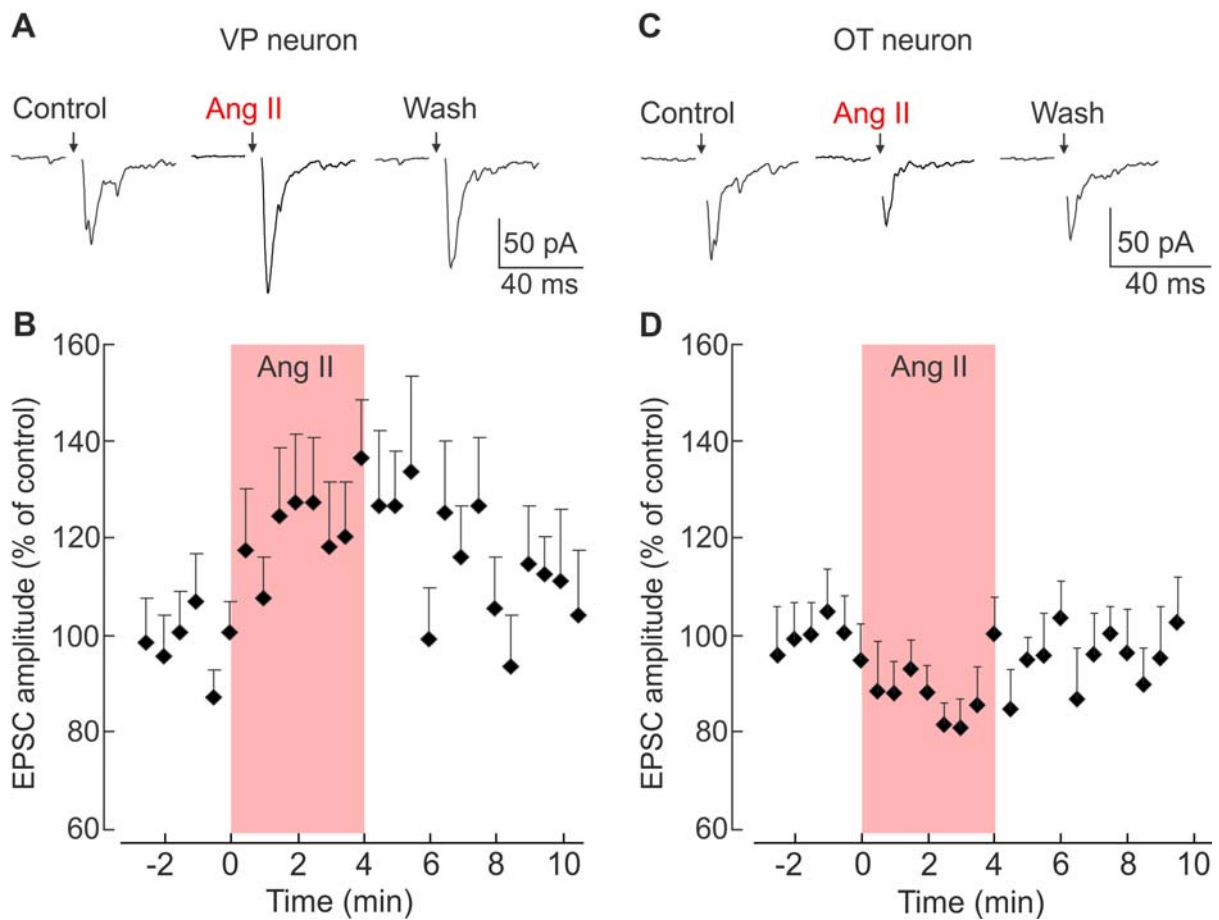


Figure S3 (related to Figure 1). Ang II causes antiparallel changes in EPSC amplitude in OT and VP neurons.

(A) Traces show EPSCs evoked in a VP neuron by electrical stimulation of the OVLT (arrow; average of 10 sweeps) in the absence (control, wash) and presence of Ang II. (B) Graph shows the effect of Ang II (shaded area) on the mean (\pm s.e.m.) normalized evoked EPSC amplitude recorded from VP neurons ($n = 12$; each point was calculated from the average of amplitude of 3 consecutive EPSCs evoked in each cell). (C) Sample current traces show the effect of Ang II on a single OT neuron (same layout as A). (D) Graph shows the effect of Ang II (shaded area) on the mean (\pm s.e.m.) normalized evoked EPSC amplitude recorded from all OT neurons ($n = 19$; layout as in B).

Figure S4

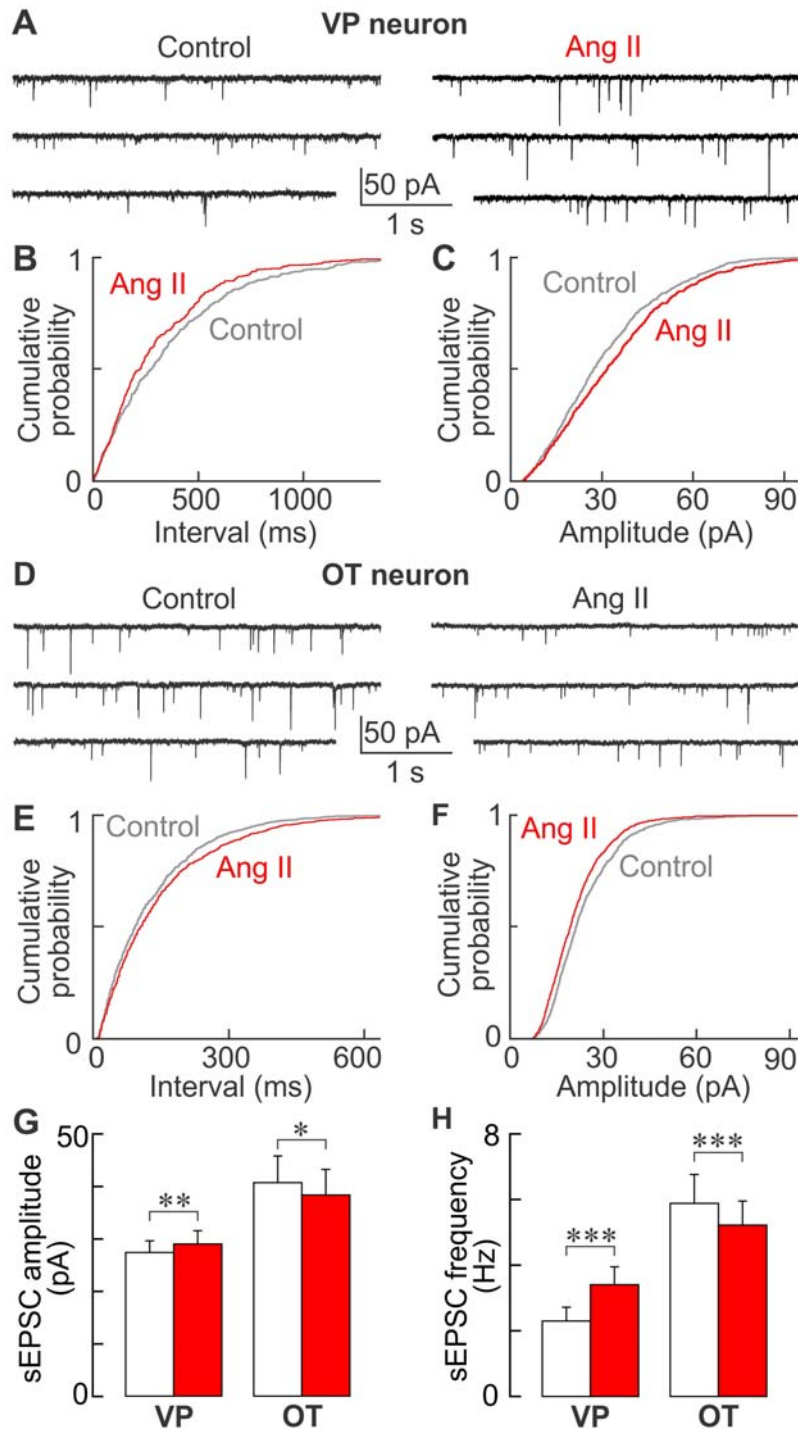


Figure S4 (related to Figure 3). Ang II causes antiparallel changes in network activity in OT and VP neurons.

(A) Traces illustrate sEPSC activity in a VP neuron before (Control) and during application of Ang II in the SON. (B) Cumulative probability plots show the distribution of sEPSC intervals recorded during control conditions (gray trace) and in the presence of Ang II (3 mins each). Note the leftward shift in the interval distribution, indicating an increase in frequency compared to control (Kolmogorov-Smirnov (KS) test; $p = 0.000004$). (C) Cumulative probability plots show the effect of Ang II on the distributions of sEPSC amplitudes in the same cell. Ang II induces a rightward shift in amplitude distribution compared to controls, indicating an increase in amplitude (KS test; $p = 0.009$). (D) Traces show representative sEPSC activity recorded in an OT neuron before (Control) and in the presence of Ang II. (E) Cumulative probability plots show the distribution of sEPSC intervals in control conditions (gray) and in the presence of Ang II (3 mins each). Ang II causes a significant rightward shift in inter-event interval distribution, indicating a reduction in frequency (KS test; $p = 0.04$). (F) Cumulative

probability plots show the effect of Ang II on the distributions of sEPSC amplitudes in the same cell. Ang II induces a leftward shift in amplitude distribution compared to control, indicating a decrease in amplitude (KS test; $p = 0.0003$). (G,H) Bar graphs plot mean (\pm s.e.m.) sEPSC amplitude (G) and frequency (H) observed in VP and OT neurons (* $p < 0.05$; ** $p < 0.01$; *** $p < 0.005$).

SUPPLEMENTAL EXPERIMENTAL PROCEDURES

Slice recordings

Angled hypothalamic slices were prepared as previously described (Stachniak et al., 2012) from male Long-Evans rats (50-80g, Charles River) or transgenic VPeGFP male and female Wistar rats (50-250g) anaesthetized with halothane, in accordance with a protocol approved by the McGill University Animal Care Committee. After extraction, brains were placed in ice-cold (0-4°C) oxygenated (5%/95% CO₂/O₂ mixture) artificial cerebrospinal fluid (ACSF; 296±2 mosmol/kg, except where indicated) containing (in mM): NaCl, 120; KCl, 3; NaH₂PO₄, 1.23; MgCl₂, 1.48; CaCl₂, 1; NaHCO₃, 25.95; and D-glucose, 10. The dorsal surface of the brain was glued to an angled (35°) mounting block and a single 400 µm slice just caudal to the optic chiasma was cut on a vibratome (Leica VT1200), transferred to a recording chamber and perfused at ~2 ml/min with 32°C oxygenated ACSF.

Recordings began ≥45 minutes after slice preparation. Cells were visualized using an Olympus BX51WI upright microscope coupled to a Photometrics (Tucson, AZ) Coolsnap cf2 digital camera using RSImage software (Roper Scientific). Electrodes were visually guided to each cell using a motorized micromanipulator (SD Instruments Inc., Grants Pass, OR). Under these conditions, pipette series resistance was 5-15 MΩ. Membrane potentials were not corrected for a liquid junction error of +2 mV. Unless otherwise stated, holding potential was -70 mV. Cell conductance and series resistance was monitored by applying a 50 mV hyperpolarizing pulse at the end of each sweep. For current clamp recordings, KMeSO₄ was used instead of K gluconate to reduce impairment of the afterhyperpolarization (Kaczorowski et al., 2007). For synaptic playback experiments, whole cell voltage was recorded on a Multiclamp 700B amplifier attached to a Digidata 1440A interface controlled with pCLAMP 10 software. For neurobiotin labeled cells, each recording was followed by a 4 minute current injection protocol in voltage clamp, consisting of an oscillating current pulse to from -70 mV to +70 mV for 500 msec at 1Hz. Recordings were excluded if the series resistance increased by more than 6 MΩ over the course of the trial, or if the holding current exceeded -200 pA at any point.

Electrical stimulation of the OVLT

Electrical stimulation of the OVLT (one trial per 10s) was performed in the presence of picrotoxin (100 μM) by passing current through a bipolar electrode embedded adjacent to the OVLT (Trudel and Bourque, 2003). Bipolar stimulating electrodes were made from a pair of teflon-coated platinum-iridium wires (50 μm o.d.; A-M Systems Inc., Everett, WA). Coating was removed for the final 250 μm of each wire. For stimulation, both wire tips were inserted into the OVLT. Stimuli (10 to 70 μA ; 0.1 to 0.5ms) were delivered via an isolated stimulator device (DS2; Digitimer Ltd., Hertfordshire, England) triggered via the acquisition system.

Application of drugs by pressure-ejection

Hyperosmotic stimuli (+20 mosmol/kg; ACSF + 20 mM mannitol) and Ang II (Phoenix Pharmaceuticals, Burlingame, CA; 10^{-5} M) were pressure-ejected via a patch pipette connected to a Multi-Channel Picospritzer (General Valve Corporation). The pipette targeting the OVLT (Hyperosmotic solution) was positioned in the parenchyma of the tissue ~ 0.2 mm rostral to the preoptic recess of the third ventricle. The pipette targeting the SON was placed just at the edge of the nucleus, upstream of the ACSF delivery tube supplying the recording chamber. Using this method drugs applied in the SON did reach the OVLT and vice versa (Trudel and Bourque, 2010). Control experiments using extracellular recordings made at various positions relative to the tip of a pressure-ejection pipette delivering either glutamate or GABA confirmed that lateral diffusion was not a significant factor beyond a radius of 200 μm from the site of injection (data not shown). With regards to Ang II, bath application of Ang II at 100 nM readily and reliably affected EPSC amplitude (data not shown). Although effects of equivalent magnitude could also be evoked by local puffing of 0.1-1 μM , a greater percentage of cells failed to respond than observed by bath application, presumably due to drug dilution or reduced cell access using this method. We therefore opted for 10 μM to maximize the reliability of Ang II effects induced by local pressure-ejection.

Identification of OT and VP neurons

VP and OT neurons are indistinguishable by visual inspection alone. However immunohistochemistry has shown that the two cell types occupy well-segregated parts of the SON in angled horizontal slices of rat hypothalamus, with rostral parts of the nucleus comprising almost exclusively OT neurons and caudal parts of the nucleus comprising almost exclusively VP

neurons (Stachniak et al., 2012). Using position as an initial guide, cell identification was confirmed using one of two other approaches. First, when using slices prepared from transgenic rats expressing enhanced green fluorescent protein (eGFP) under the control of the vasopressin promoter (VPeGFP rats) (Ueta et al., 2005), VP neurons could be directly identified by epifluorescence using a mercury lamp (Olympus, Model No. BH2-RFL-T3) and a green filter cube (Olympus, U-MNB2). Putative OT neurons were identified based on absence of eGFP combined with an extreme rostral position (Stachniak et al., 2012). Otherwise, OT and VP neurons were identified by post-hoc immunohistochemistry in slices containing cells that were injected with neurobiotin during the recording. In the latter case, 1 cell per slice was recorded and its relative position in the nucleus noted. Primary antibodies included PS-41, a mouse monoclonal antibody directed against vasopressin-associated neurophysin (1:25); and VA-10, a rabbit polyclonal antibody directed against oxytocin-associated neurophysin (1:250) (Altstein et al., 1988; Ben Barak et al., 1985), secondary antibodies were labeled goat anti-mouse (Alexa Fluor 488, 1:200, Invitrogen A11001), anti-rabbit (Alexa Fluor 568, 1:200, Invitrogen A11011), and AMCA avidin (1:500, Vector A-2008). Neurobiotin/immunolabeled cells were visualized using RSIImage software (Roper Scientific) connected to an Olympus IX71 microscope attached to a Lambda DG-4 fluorescence unit (Sutter).

Analysis of firing rates during hypertonic stimulation of the OVLT

For osmotic stimulation experiments, basal cell firing rates were initially adjusted to around 3 Hz by adjusting the amount of DC current being injected (generally less than ± 10 pA) and the firing rate was left to stabilize for > 1 min before the test. Basal firing frequencies ranged from about 0.5-6 Hz. Following Ang II application the cells were excited. Once this effect had stabilized (~ 60 s), firing rate was readjusted to a value near the original baseline by injection of hyperpolarizing current (0.1-5 pA). The effect of a hyperosmotic stimulus to the OVLT was then re-examined in the continuous presence of Ang II in the SON. Firing frequency was analyzed in 30 seconds periods, just prior to hyperosmotic puff onset (baseline) and 10 to 40 seconds after onset. Cells were excluded from analysis if they showed no response to a hyperosmotic puff under any condition ($\Delta\text{Hz} < 0.15$ Hz), if spike rates were not stable during the baseline period, or if baseline frequency in the presence and absence of Ang II differed by more than 1.5 Hz.

Analysis of evoked EPSCs

To measure EPSC amplitudes, all of the EPSCs evoked in a particular cell were first averaged together to clearly determine the position of the peak of the EPSC and cursors were placed on either side of this peak. The amplitude of each individual evoked EPSC was then measured as the average of all points included within this fixed window, minus the baseline holding current before the corresponding sweep. For each cell, a “Control” EPSC amplitude was determined as the average of 12 EPSCs recorded before applying Ang II, and the effect of the peptide was measured as the average amplitude of the last 12 EPSCs recorded in the presence of Ang II.

To measure synaptically-evoked charge transfer (ΔQ), a first pair of cursors (10 ms apart) was placed before the stimulus to measure baseline current (I_{baseline}) and a second pair of cursors was positioned to span the evoked response. The first cursor was placed before the rising phase of the EPSC (after the stimulus artefact had returned to baseline) and a second cursor was placed ~50 ms later. Therefore the mean evoked current (I_{evoked}) recorded this way captured the bulk of the current carried by the synchronous component of the evoked EPSC together with asynchronous events (aEPSCs) evoked by the stimulus. The value of ΔQ was determined from the average synaptically evoked current ($I_{\text{evoked}} - I_{\text{baseline}}$) multiplied by the duration of the second cursor window.

For PPR analysis, cells were excluded if they showed PPR values of less than 0.1 or greater than 10. For failure analysis, any evoked EPSC amplitude less than 5 pA was considered a failure.

Spontaneous EPSCs (sEPSCs) were recorded under isotonic or hypertonic conditions (to increase the proportion of OVLT mediated events), and detected using the template match function of Clampfit 10. Detected synaptic event amplitudes and inter-event intervals (IEI, ~3 min each) were subjected to a Kolmogorov-Smirnov analysis. Series resistance was less than 20 M Ω , and did not vary by more than 3 M Ω .

SUPPLEMENTAL REFERENCES

Altstein, M., Whitnall, M.H., House, S., Key, S., and Gainer, H. (1988). An immunochemical analysis of oxytocin and vasopressin prohormone processing in vivo. *Peptides* 9, 87-105.

Ben Barak, Y., Russell, J.T., Whitnall, M.H., Ozato, K., and Gainer, H. (1985). Neurophysin in the hypothalamo-neurohypophysial system. I. Production and characterization of monoclonal antibodies. *J Neurosci* 5, 81-97.

Kaczorowski, C.C., Disterhoft, J., and Spruston, N. (2007). Stability and plasticity of intrinsic membrane properties in hippocampal CA1 pyramidal neurons: effects of internal anions. *J Physiol* 578, 799-818.

Stachniak, T.J., Sudbury, J.R., Trudel, E., Choe, K.Y., Ciura, S., and Bourque, C.W. (2012). Osmoregulatory circuits in slices and en-bloc preparations of rodent hypothalamus. In *Isolated Central Nervous System Circuits*, B. K., ed. (New York: Humana-Springer).

Trudel, E., and Bourque, C.W. (2003). A rat brain slice preserving synaptic connections between neurons of the suprachiasmatic nucleus, organum vasculosum lamina terminalis and supraoptic nucleus. *J Neurosci Methods* 128, 67-77.

Trudel, E., and Bourque, C.W. (2010). Central clock excites vasopressin neurons by waking osmosensory afferents during late sleep. *Nat Neurosci* 13, 467-474.

Ueta, Y., Fujihara, H., Serino, R., Dayanithi, G., Ozawa, H., Matsuda, K.i., Kawata, M., Yamada, J., Ueno, S., Fukuda, A., and Murphy, D. (2005). Transgenic Expression of Enhanced Green Fluorescent Protein Enables Direct Visualization for Physiological Studies of Vasopressin Neurons and Isolated Nerve Terminals of the Rat. *Endocrinology* 146, 406-413.